6812 *Inorg. Chem.* **2009**, *48*, 6812–6822
DOI: 10.1021/ic900761u

Inorganic Chemistry
Article

Mono- and Bis- Methyltrioxorhenium(VII) Complexes with Salen Ligands: Synthesis, Properties, Applications

Zhaoqing Xu,[†] Ming-Dong Zhou,[‡] Markus Drees,[†] Hugh Chaffey-Millar,[‡] Eberhardt Herdtweck,[†] Wolfgang A. Herrmann,[†] and Fritz E. Kühn*[,†,‡]

[†]*Chair of Inorganic Chemistry, and* [‡]*Molecular Catalysis, Catalysis Research Center, Technische Universität München, Lichtenbergstrasse 4, D-85747 Garching bei München, Germany*

Received April 20, 2009

Methyltrioxorhenium(VII) (MTO) forms 1:1 (mono-) or/and 2:1 (bis-) complexes with salen ligands, undergoing a hydrogen transfer from a ligand-bound OH-group to a ligand nitrogen atom. Some complexes show good stability both in the solid state and in solution, while others must be kept at low temperatures under an argon atmosphere. X-ray crystallography shows distorted trigonal bipyramidal structures of all examined complexes in the solid state, this structure being due to the steric demands of the ligands, with the methyl group of MTO residing in the apical sites in the cis position. Temperature-dependent proton NMR data indicate that the coordination between salen ligands and MTO at low temperatures is considerably stronger than at room temperature. Density functional theory calculations have been performed to find approximate structures for all described complexes and to try to find a rationale for the preferred formation of mono- versus bis-MTO complexes. The formation of mono- or bis-MTO adducts is dependent on both the steric and the electronic influence of the respective salen ligands. The catalytic performance is strongly influenced by the ring substitution. Two MTO molecules coordinated to one salen ligand lead to an additional boost of catalytic activity because there is not only double the amount of catalytic centers present but also a "ligand enhanced" activity increase.

Introduction

When methyltrioxorhenium (MTO) was first described in the literature 30 years ago, it was considered as just another curiosity in organometallic chemistry.[1] More than a decade later, its great potential as a catalyst for a plethora of organic reactions was discovered.[2] Beyond that, the interesting properties of polymeric MTO in material science were found,[3] and efficient and benign ways to synthesize this versatile compound were developed.[4] The reaction chemistry of MTO is, nevertheless, still largely dominated by its catalytic applications.[5] Lewis base adducts, for example, became of much greater interest after it was discovered that MTO/pyridine mixtures are significantly more selective and efficient catalysts in olefin epoxidation than MTO itself.[6] Since then, much effort has been dedicated to the identification of MTO complexes with

*To whom correspondence should be addressed. E-mail: fritz.kuehn@ch.tum.de. Fax: + 49 89 289 13473.

(1) Beattie, I. R.; Jones, P. J. *Inorg. Chem.* **1979**, *18*, 2318–2319.

(2) (a) Herrmann, W. A.; Wang, M. *Angew. Chem., Int. Ed. Engl.* **1991**, *30*, 1641–1643. (b) Herrmann, W. A.; Fischer, R. W.; Marz, D. W. *Angew. Chem., Int. Ed. Engl.* **1991**, *30*, 1638–1641. (c) Herrmann, W. A.; Wagner, W.; Flessner, U. N.; Volkhardt, U.; Komber, H. *Angew. Chem., Int. Ed. Engl.* **1991**, *30*, 1636–1638.

(3) (a) Genin, H. S.; Lawler, K. A.; Hoffmann, R.; Herrmann, W. A.; Fischer, R. W.; Scherer, W. *J. Am. Chem. Soc.* **1995**, *117*, 3244–3252. (b) Herrmann, W. A.; Scherer, W. R.; Fischer, W.; Blümel, J.; Kleine, M.; Mertin, W.; Gruehn, R.; Mink, J.; Boysen, H.; Wilson, C. C.; Ibberson, R. M.; Bachmann, L.; Mattner, M. *J. Am. Chem. Soc.* **1995**, *117*, 3231–3243. (c) Miller, R.; Helbig, C.; Eickerling, G.; Herrmann, R.; Scheidt, E. W.; Scherer, W. *Phys. B (Amsterdam, Neth.)* **2005**, *359*, 448–450. (d) Helbig, C.; Herrmann, R.; Mayr, F.; Scheidt, E. W.; Troster, K.; Hanss, J.; Nidda, H. A. K. v.; Heymann, G.; Hupperz, H.; Scherer, W. *Chem. Commun.* **2005**, 4071–4073. (e) Miller, R.; Scheidt, E. W.; Eickerling, G.; Helbig, C.; Mayr, F.; Herrmann, R.; Scherer, W.; H. Nidda, A. K. v.; Eyert, V.; Schwab, P. *Phys. Rev. B*, **2006**, *73*, Art. Nr. 165113. (f) Scheidt, E. W.; Miller, R.; Eickerling, G.; Mayr, F.; Herrmann, R.; Schwab, P.; Scherer, W. *Phys. B (Amsterdam, Neth.)* **2006**, *378*−*380*, 1132–1133. (g) Herrmann, R.; Troster, K.; Eickerling, G.; Helbig, C.; Hauf, C.; Miller, R.; Mayr, F.; H.; Nidda, A. K. v.; Scheidt, E. W.; Scherer, W. *Inorg. Chim. Acta* **2006**, *359*, 4779–4788. (h) Simone, M.; Coreno, M.; Green, J. C.; McGrady, S.; Pritchard, H. *Inorg. Chem.* **2003**, *42*, 1908–1918.

(4) (a) Herrmann, W. A.; Kuchler, J. G.; Felixberger, J. K.; Herdtweck, E.; Wagner, W. *Angew. Chem., Int. Ed. Engl.* **1988**, *27*, 394–396. (b) Herrmann, W. A.; Kühn, F. E.; Fischer, R. W.; Thiel, W. R.; Romão, C. C. *Inorg. Chem.* **1992**, *31*, 4431–4432. (c) Herrmann, W. A.; Kratzer, R. M.; Fischer, R. W. *Angew. Chem., Int. Ed. Engl.* **1997**, *36*, 2652–2654. (d) Herrmann, W. A.; Rost, A. M. J.; Mitterpleininger, J. K. M.; Szesni, N.; Sturm, S.; Fischer, R. W.; Kühn, F. E. *Angew. Chem., Int. Ed. Engl.* **2007**, *46*, 7301–7303. (e) Tosh, E.; Mitterpleininger, J. M. K.; Rost, A. M. J.; Veljanovski, D.; Herrmann, W. A.; Kühn, F. E. *Green Chem.* **2007**, *9*, 1296–1298. (f) Mitterpleininger, J. M. K.; Szesi, N.; Sturm, S.; Fischer, R. W.; Kühn, F. E. *Eur. J. Inorg. Chem.* **2008**, *25*, 3929–3934.

(5) (a) Romão, C. C.; Kühn, F. E.; Herrmann, W. A. *Chem. Rev.* **1997**, *97*, 3197–3246. (b) Kühn, F. E.; Jain, K. R.; Zhou, M. D. *Rare Met.* **2006**, *359*, 411–421. (c) Rost, A. M. J.; Herrmann, W. A.; Kühn, F. E. *Tetrahedron Lett.* **2007**, *48*, 1775–1779. (d) Jain, K. R.; Kühn, F. E. *J. Organomet. Chem.* **2007**, *692*, 5532–5540.

(6) (a) Rudolph, J. K.; Reddy, L.; Chiang, J. P.; Sharpless, K. B. *J. Am. Chem. Soc.* **1997**, *119*, 6189–6190. (b) Coperet, C.; Adolfsson, H.; Sharpless, K. B. *Chem. Commun.* **1997**, *16*, 1565–1566. (c) Coperet, C.; Adolfsson, H.; Khuong, T. A. V.; Yudin, A. K.; Sharpless, K. B. *J. Org. Chem.* **1998**, *63*, 1740–1741. (d) Adolfsson, H.; Converso, A.; Sharpless, K. B. *Tetrahedron Lett.* **1999**, *40*, 3991–3994.

Published on Web 06/23/2009

greater catalytic efficiency than those already known—a quest that led to the description of mono-[7] and bidentate[8] Lewis base adducts of MTO as well as to Schiff-base adducts[9] and polymer coordinated MTO.[10] Kinetic and thermodynamic studies have been performed to understand the formation, stability, and catalytic behavior of such systems.[11] Except for the polymer bound complexes, usually only one MTO moiety (as an electron acceptor) is associated with one electron donor moiety. The binding of a second MTO molecule to bi- and tetradendate Lewis bases has proven to be largely unsuccessful. Only very few such complexes are described in the literature, and the rarity of such compounds has been largely ascribed to the fact that the electron withdrawing ability of MTO rarely allows a second Lewis acid to coordinate in close proximity to MTO on a donor moiety.[7,8,12] Additionally, heteronuclear complexes with MTO as an electron acceptor and another metal complex (in a low oxidation state) as a donor, are equally uncommon.[13]

In this work, salen ligands have been investigated for their potential as being able to bind two MTO molecules. Despite their widespread use in transition metal complexes (among them several Re compounds[14]), salen ligands had not yet been applied in the coordination of MTO. In contrast to the previous examined N-base ligands, which have to be applied in significant excess with respect to MTO to reach full potential in epoxidation catalysis[6−8] and to Schiff base ligands that can be used in a 1:1 fashion,[9] salen ligands are potentially able to bind two MTO molecules per ligand. In the experiments, when MTO is treated with a stoichiometric amount of a salen ligand synthesized from ethylene diamine and salicylic aldehyde, the stable 1:1 MTO salen complex **1** is obtained. In comparison to many *N*-coordinated Lewis base adducts, which are considerably more sensitive to the presence of moisture and temperature than MTO itself,[15] compound **1** shows good stability at room temperature both in the solid state and in solution. By simply changing the ratio of metal to ligand to 2:1, the MTO salen complex **5**, which has two MTO units in its structure, can easily be prepared. In this work, the synthesis of a series of mono- and bis- MTO salen complexes is reported with their stabilities and behavior being examined, compared, and interpreted.

Experimental Section

Synthetic Methods and Characterization Data. All preparations and manipulations were performed using standard Schlenk techniques under an atmosphere of argon. Solvents were dried by standard procedures (*n*-hexane and Et_2O over Na; CH_2Cl_2 over CaH_2), distilled under argon and used immediately. Microanalyses of the obtained products were performed in the Mikroanalytisches Labor of the Technical University of Munich in Garching. Mid-IR spectra were measured on Bio-Rad FTS 525 spectrometer using KBr pellets. ^{1}H and ^{13}C NMR obtained using a 400-MHz Bruker Avance DPX-400 spectrometer. Catalytic runs were monitored by gas chromatography (GC) methods on a Hewlett-Packard instrument HP 5890 Series II equipped with a FID, a Supelco column Alphadex 120, a Chiraldex capillary column Alltech GBP and a Hewlett-Packard integration unit HP 3396 Series II. CI-MS spectra (isobutene as CI gas) were obtained on a Finnigan MAT 90 mass spectrometer. The salen compounds were prepared in the same manner as described previously.[16] MTO was synthesized according to literature procedures.[17]

Preparation of Complexes 1−4. A solution of CH_3ReO_3 (0.25 g, 1 mmol) in Et_2O (3 mL) was added dropwise to a stirred solution of ligand (see Scheme 1; 1 mmol in 3 mL of Et_2O) at 23 °C. The system was stirred for 30 min. Subsequently, the yellow solution was concentrated to approximately 0.5 mL under an oil pump vacuum, and 6 mL of dry *n*-hexane was added and the system cooled to 0 °C. The yellow precipitate was collected by filtration, washed with *n*-hexane, and dried under reduced pressure.

Complex 1. Color: yellow. Yield: 82%. $C_{21}H_{25}N_2O_5Re$ (571.64), elemental analysis calcd.(%): C, 44.12; H, 4.41; N, 4.90; found: C, 44.57; H, 4.40; N, 4.98; ^{1}H NMR (400 MHz, $CDCl_3$, rt): δ 13.13 (2H, s, OH), 8.25 (2H, s, CH = N), 7.26−7.22 (2H, m, ArH), 7.14 (2H, dd, J = 8, ArH), 6.89 (2H, t, J = 7, ArH), 6.78 (2H, t, J = 7, ArH), 3.37−3.31 (2H, m, CHN), 2.58 (3H, s, CH_3Re), 1.98−1.87 (4H, m, CH_2), 1.77−1.68 (2H, m, CH_2), 1.50−1.45 ppm (2H, m, CH_2); ^{13}C NMR (100 MHz, $CDCl_3$, rt): δ 164.9 (C=N), 161.5 (C_{Ar}), 132.2 (C_{Ar}), 131.7 (C_{Ar}), 118.6 (C_{Ar}), 117.0 (C_{Ar}), 72.4 (CN), 33.1 (CH_2), 24.2 (CH_2), and 19.7 ppm (CH_3Re); IR (KBr): see Tables 2 and 3; MS (CI): m/z (%) 251.0 (MTO + H^+, 62.14), 323.1 (MH^+ − MTO^+, 90.1).

Complex 2. Color: yellow. Yield: 80%. $C_{29}H_{41}N_2O_5Re$ (683.85), elemental analysis calcd.(%): C, 50.93; H, 6.04; N, 4.10; found: C, 50.89; H, 6.23; N, 3.98; ^{1}H NMR (400 MHz, $CDCl_3$, rt): δ 13.11 (2H, s, OH), 8.24 (2H, s, CH = N), 7.29−7.25 (2H, m, ArH), 7.11 (2H, d, J = 2, ArH), 6.82 (2H, d, J = 9, ArH), 3.31 (2H, m, CHN), 2.54 (3H, s, CH_3Re), 1.94−1.86 (4H, m, CH_2), 1.73−1.70 (2H, m, CH_2), 1.49−1.44 (2H, m, CH_2), 1.18 ppm (18H, s, $C(CH_3)_3$); ^{13}C NMR (100 MHz, $CDCl_3$, rt): δ 165.4 (C=N), 159.6 (C_{Ar}), 141.2 (C_{Ar}), 130.2 (C_{Ar}), 128.2 (C_{Ar}), 117.8 (C_{Ar}), 116.7 (C_{Ar}), 72.3 (CN), 34.0 (CCH_3), 33.2 (CH_2), 31.4 (CH_3), 24.2 (CH_2), and 20.2 ppm

(7) Kühn, F. E.; Santos, A. M.; Roesky, P. W.; Herdtweck, E.; Scherer, W.; Gisdakis, P.; Yudanov, I. V.; Valentin, C. Di; Rösch, N. *Chem.—Eur. J.* **1999**, *5*, 3603–3615.

(8) Ferreira, P.; Xue, W. M.; Bencze, E.; Herdtweck, E.; Kühn, F. E. *Inorg. Chem.* **2001**, *40*, 5834–5841.

(9) (a) Zhou, M.; Zhao, J.; Li, J.; Yue, S.; Bao, C.; Mink, J.; Zang, S.; Kühn, F. E. *Chem.—Eur. J.* **2007**, *13*, 158–166. (b) Zhou, M. D.; Zang, S. L.; Herdtweck, E.; Kühn, F. E. *J. Organomet. Chem.* **2008**, *693*, 2473–2477. (c) Capapé, A.; Zhou, M. D.; Zang, S. L.; Kühn, F. E. *J. Organomet. Chem.* **2008**, *693*, 3240–3244.

(10) Gonzales, L.; Villa, A. L.; Montes, C. *React. Funct. Polym.* **2005**, *65*, 169–181.

(11) (a) Wang, W. D.; Espenson, J. H. *J. Am. Chem. Soc.* **1998**, *120*, 11335–11341. (b) Nabavizadeh, S. M. *Inorg. Chem.* **2003**, *42*, 4204–4208. (c) Nabavizadeh, S. M.; Akbari, A.; Rashidi, M. *Eur. J. Inorg. Chem.* **2005**, 2368–2375. (d) Nabavizadeh, S. M. *Dalton Trans.* **2005**, 1644–1648. (e) Nabavizadeh, S. M.; Akbari, A.; Rashidi, M. *Dalton Trans.* **2005**, 2423–2427. (f) Nabazvizadeh, S. M.; Rashidi, M. *J. Am. Chem. Soc.* **2006**, *128*, 351–357.

(12) (a) Herrmann, W. A.; Weichselbaumer, G.; Herdtweck, E. *J. Organomet. Chem.* **1989**, *372*, 371–389. (b) Rietveld, M. H. P.; Nagelholt, L.; Grove, D. M.; Veldman, N.; Spek, A. L.; Rauch, M. U.; Herrmann, W. A.; Koten, G. v. *J. Organomet. Chem.* **1997**, *530*, 159–167.

(13) (a) Santos, A. M.; Kühn, F. E.; Xue, W.-M.; Herdtweck, E. *J. Chem. Soc., Dalton Trans.* **2000**, *20*, 3570–3574. (b) Cunha-Silva, L.; Gonçalves, I. S.; Pillinger, M.; Xue, W.-M.; Rocha, J.; Teixeira-Dias, J. J. C.; Kühn, F. E. *J. Organomet. Chem.* **2002**, *656*, 281–287.

(14) (a) Kühn, F. E.; Rauch, M. U.; Lobmaier, G. M.; Artus, G. R. J.; Herrmann, W. A. *Chem. Ber.−Recueil* **1997**, *130*, 1427–1431. (b) Bommel, K. J. C. v.; Verboom, W.; Kooijlman, H.; Spek, A. L.; Reinhoudt, D. N. *Inorg. Chem.* **1997**, *37*, 4197–4203. (c) Ison, E. A.; Cessarich, J. E.; Travia, N. E.; Fanwick, P. E.; Abu-Omar, M. M. *J. Am. Chem. Soc.* **2007**, *129*, 1167–1178. (d) Pointillart, F.; Bernot, K.; Sessoli, R. *Inorg. Chem. Commun.* **2007**, *10*, 471–474. (e) Du, G.; Fanwick, P. E.; Abu-Omar, M. M. *Inorg. Chim. Acta* **2008**, *361*, 3184–3192.

(15) (a) Herrmann, W. A.; Kiprof, P.; Rybdal, K.; Tremmel, J.; Blom, R.; Alberto, R.; Behm, J.; Albach, R. W.; Bock, H.; Solouki, B.; Mink, J.; Lichtenberger, D.; Gruhn, N. E. *J. Am. Chem. Soc.* **1991**, *113*, 6527–6537. (b) Herrmann, W. A.; Fischer, R. W.; Rauch, M. U.; Scherer, W. *J. Mol. Catal.* **1994**, *86*, 243–266. (c) Rudler, H.; Gregorio, J. R.; Denise, B.; Bregeault, J. M.; Deloffre, A. *J. Mol. Catal. A* **1998**, *133*, 255–265. (d) Saladino, R.; Andreoni, A.; Neri, V.; Crestini, C. *Tetrahedron* **2005**, *61*, 1069–1075. (e) Yamazaki, S. *Org. Biomol. Chem.* **2007**, *5*, 2109–2113. (f) Yamazaki, S. *Tetrahedron* **2008**, *64*, 9253–9257.

(16) (a) Lopez, J.; Liang, S.; Ru, X. R. *Tetrahedron Lett.* **1998**, *39*, 4199–4202. (b) Boghaei, D. M.; Mohebi, S. *J. Mol. Catal. A: Chem.* **2002**, *179*, 41–51. (c) Lin, B.-B.; Qiu, Y.-Q.; Su, Z.-M.; Sun, S.-L.; Feng, J.-K. *Chem. J. Chin. Univ.* **2001**, *22*, 1551–1554.

(17) Tosh, E.; Mitterpleininger, H. K. M.; Rost, A. M. J.; Veljanovski, D.; Herrmann, W. A.; Kühn, F. E. *Green Chem.* **2007**, *12*, 1296–1298.

Scheme 1. Synthesis of MTO Salen Complexes **1**−**7**

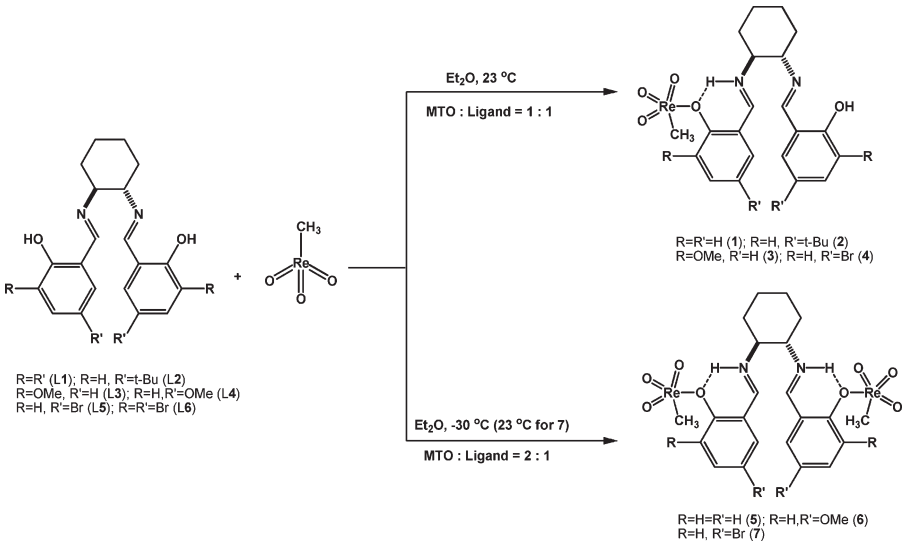

(CH_3Re); IR (KBr): see Tables 2 and 3; MS (CI): *m*/*z* (%) 251.0 ($MTO + H^+$, 84.45), 435.2 ($MH^+ - MTO^+$, 100).

Complex 3. Color: yellow. Yield: 90%. $C_{23}H_{29}N_2O_7Re$ (631.69), elemental analysis calcd.(%): C, 43.73; H, 4.63; N, 4.43; found: C, 43.60; H, 4.69; N, 4.60; ^1H NMR (400 MHz, $CDCl_3$, rt): δ 13.82 (2H, s, OH), 8.23 (2H, s, CH = N), 6.87−6.69 (6H, m, ArH), 3.85 (6H, s, OCH_3) 3.32−3.29 (2H, m, CHN), 2.59 (3H, s, CH_3Re), 1.95−1.86 (4H, m, CH_2), 1.74−1.69 (2H, m, CH_2), 1.50−1.45 ppm (2H, m, CH_2); ^{13}C NMR (100 MHz, $CDCl_3$, rt): δ 164.8 (C═N), 151.7 (C_{Ar}), 148.4 (C_{Ar}), 123.3 (C_{Ar}) 118.4 (C_{Ar}), 117.9 (C_{Ar}), 114.0 (C_{Ar}), 72.4 (CN), 56.1 (OCH_3), 33.1 (CH_2), 24.1 (CH_2), and 19.5 ppm (CH_3Re); IR (KBr): see Tables 2 and 3; MS (CI): *m*/*z* (%) 249.2 (MTO^+, 12.48), 383.1 ($MH^+ - MTO^+$, 100).

Complex 4. Color: yellow. Yield: 74%. $C_{21}H_{23}Br_2N_2O_5Re$ (729.43), elemental analysis calcd.(%): C, 38.83; H, 3.57; N, 4.31; found: C, 38.82; H, 3.64; N, 4.12; ^1H NMR (400 MHz, $CDCl_3$, rt): δ 13.22 (2H, s, OH), 8.17 (2H, s, CH = N), 7.33 (2H, d, *J* = 2.5, ArH), 7.31 (2H, d, *J* = 2.4, ArH), 6.81−6.78 (2H, d, *J* = 8.8, ArH), 3.33 (2H, m, CHN), 2.60 (3H, s, CH_3Re), 1.95−1.88 (4H, m, CH_2), 1.75−1.67 (2H, m, CH_2), 1.50−1.45 ppm (2H, m, CH_2); ^{13}C NMR (100 MHz, $CDCl_3$, rt): δ 163.5 (C═N), 160.0 (C_{Ar}), 135.0 (C_{Ar}), 133.5 (C_{Ar}) 120.0 (C_{Ar}), 119.0 (C_{Ar}), 110.1 (C_{Ar}), 72.7 (CN), 33.0 (CH_2), 24.1 (CH_2), and 19.5 ppm (CH_3Re); IR (KBr): see Tables 2 and 3; MS (CI): *m*/*z* (%) 251.0 ($MTO + H^+$, 18.49), 480.5 ($M^+ - 2MTO^+$, 54.16), 717.5 ($(MH^+ + 2) - CH_3^+$, 12.32), 732.4 ($MH^+ + 2$, 7.24).

Preparation of Complexes 5−**7.** A solution of CH_3ReO_3 (0.25 g, 1 mmol) in Et_2O (3 mL) was added dropwise to a stirred solution of ligand (see Scheme 1; 0.5 mmol in 1.5 mL of Et_2O) at −30 °C (for **5** and **6**) and 23 °C (for **7**). The system was stirred for 30 min. The reaction solutions for **5** and **6** were gradually warmed to room temperature. The yellow solution was then concentrated to about 0.5 mL under an oil pump vacuum, and 6 mL of dry *n*-hexane was added and the system was cooled to 0 °C. The precipitate was collected by filtration, washed with *n*-hexane, and dried under reduced pressure.

The enantiomerically pure complex **7** was synthesized from (1*S*,2*S*)-(+)-1,2-diaminocyclohexane by the same procedure as described above.

Complex 5. Color: yellow-green. Yield: 83%. $C_{22}H_{28}N_2O_8Re_2$ (820.88), elemental analysis calcd.(%): C, 30.15; H, 3.54; N, 3.52; found: C, 30.04; H, 3.68; N, 3.32; ^1H NMR (400 MHz, $CDCl_3$, rt): δ 13.30 (2H, s, OH), 8.25 (2H, s, CH = N), 7.24−7.22 (2H, m, ArH), 7.15−7.13 (2H, d, *J* = 7.6, ArH), 6.89−6.87 (2H, d, *J* = 8, ArH), 6.79 (2H, t, *J* = 8.3, ArH), 3.34−3.31 (2H, m, CHN), 2.61 (6H, s, 2 × CH_3Re), 1.97−1.88 (4H, m, CH_2), 1.77−1.69 (2H, m, CH_2), 1.51−1.45 ppm (2H, m, CH_2); ^{13}C NMR (100 MHz, $CDCl_3$, rt): δ 164.8 (C═N), 161.4 (C_{Ar}), 132.1 (C_{Ar}), 131.7 (C_{Ar}) 118.5 (C_{Ar}), 117.0 (C_{Ar}), 72.3 (CN), 33.1 (CH_2), 24.2 (CH_2) and 19.4 ppm (CH_3Re); IR (KBr): see Table 2 and 3; MS (CI): *m*/*z* (%) 251.0 ($MTO + H^+$, 68.95), 322.7 ($MH^+ - 2MTO^+$, 100), 568.9 ($(MH^+ - MTO) - CH_3$, 3.25^+).

Complex 6. Color: red. Yield: 85%. $C_{24}H_{32}N_2O_{10}Re_2$ (880.94), elemental analysis calcd.(%): C, 32.72; H, 3.66; N, 3.18; found: C, 32.77; H, 3.68; N, 3.18; ^1H NMR (400 MHz, $CDCl_3$, rt): δ 12.77 (2H, s, OH), 8.18 (2H, s, CH = N), 6.84−6.41 (4H, m, ArH), 6.63 (2H, t, *J* = 3, ArH), 3.69 (6H, s, OCH_3), 3.30 (2H, m, CHN), 2.59 (6H, s, 2 × CH_3Re), 1.96−1.87 (4H, m, CH_2), 1.77−1.68 (2H, m, CH_2), 1.56−1.47 ppm (2H, m, CH_2); ^{13}C NMR (100 MHz, $CDCl_3$, rt): δ 164.6 (C═N), 155.3 (C_{Ar}), 152.1 (C_{Ar}), 119.5 (C_{Ar}), 118.3 (C_{Ar}), 117.5 (C_{Ar}), 114.9 (C_{Ar}), 72.7 (CN), 56.0 (OCH_3), 33.1 (CH_2), 24.2 (CH_2), and 19.6 ppm (CH_3Re); IR (KBr): see Table 2 and 3; MS (CI): *m*/*z* (%) 249.2 (MTO^+, 6.19), 383.1 ($MH^+ - MTO^+$, 100).

Complex 7. Color: yellow. Yield: 90%. $C_{22}H_{26}Br_2N_2O_8Re_2$ (978.67), elemental analysis calcd.(%): C, 27.00; H, 2.68; N, 2.86; found: C, 27.31; H, 2.83; N, 2.80; ^1H NMR (400 MHz, $CDCl_3$, rt): δ 13.22 (2H, s, OH), 8.16 (2H, s, CH = N), 7.33−7.30 (2H, m, ArH), 7.25 (2H, s, ArH), 6.78 (2H, d, *J* = 9, ArH), 3.32 (2H, m, CHN), 2.60 (6H, s, 2 × CH_3Re), 1.94−1.87 (4H, m, CH_2), 1.75−1.67 (2H, m, CH_2), 1.49−1.44 ppm (2H, m, CH_2); ^{13}C NMR (100 MHz, $CDCl_3$, rt): δ 163.6 (C═N), 160.2 (C_{Ar}), 135.1 (C_{Ar}), 133.6 (C_{Ar}), 120.0 (C_{Ar}), 119.0 (C_{Ar}), 110.2 (C_{Ar}), 72.7 (CN), 33.0 (CH_2), 24.1 (CH_2), and 19.5 ppm (CH_3Re); IR (KBr): see Table 2 and 3; MS (CI): *m*/*z* (%) 251.0 ($MTO + H^+$, 100), 481.8 ($(M^+ - 2MTO) + 2^+$, 3.86), 715.5 ($(M^+ - MTO) - CH_3^+$, 8.32), 730.5 ($M^+ - MTO^+$, 1.05).

X-ray Single Crystal Structure Determination of Complexes 1, 6, and 7. Details of the X-ray experiment, crystal parameters, data collection, and refinements are summarized in Table 1. General: Preliminary examinations and data collection were carried out on area detecting systems (**1**: Oxford Xcalibur κ-CCD device; **6** and **7**: Stoe IPDS 2T;) at the window of a sealed tube (**1**) and a rotating anode (Nonius 591) (**6** and **7**) and graphite monochromated Mo Kα radiation (λ = 0.71073 Å). Data collection was performed at (153, 173, 173) K (Oxford Cryosystems cooling device). Reflections were integrated, corrected for Lorentz, polarization, absorption effects, and arising from the scaling procedure for latent decay. The structures were solved by a combination of direct methods and difference Fourier syntheses. All non-hydrogen atoms were refined with anisotropic displacement parameters. All hydrogen atoms were calculated in ideal positions (riding model, d_{N-H} = 0.88 Å and d_{C-H} = 0.95, 0.98, 0.99, and 1.00 Å). Isotropic displacement

Table 1. X-ray Crystal Data, Data Collection Parameters, and Refinement Parameters of compounds **1**, **6**, and **7**

compound	**1**	**6**	**7**
empirical formula	$C_{21}H_{25}N_2O_5Re$	$C_{24}H_{32}N_2O_{10}Re_2$	$C_{22}H_{26}Br_2N_2O_8Re_2$
formula weight	571.64	880.94	978.67
color/habit	yellow/prism	red/column	yellow/fragment
crystal dimensions mm	0.36 × 0.38 × 0.56	0.15 × 0.15 × 0.51	0.05 × 0.30 × 0.55
crystal system	monoclinic	monoclinic	monoclinic
space group	$P2_1/n$ (No.14)	$C2/c$ (No.15)	$C2/c$ (No.15)
a, Å	12.9223(6)	18.8092(9)	27.6278(13)
b, Å	11.0773(5)	12.6315(6)	8.7700(2)
c, Å	14.9878(7)	12.9568(6)	24.9535(12)
β, deg	101.990(4)	115.555(4)	116.257(3)
V, Å^3	2098.61(17)	2777.2(2)	5422.3(4)
Z	4	4	8
D_{calcd} g cm^{-3}	1.809	2.107	2.398
absorption coefficient mm^{-1}	5.825	8.766	11.916
$F(000)$	1120	1680	3648
θ range, deg	3.0 to 25.4	4.8 to 25.4	4.7 to 25.3
no. of reflections collected	35981	20762	34454
no. of independent reflections/R_{int}	3838/0.141	2530/0.047	4893/0.059
no. of observed reflections $I > 2\sigma(I)$	3382	2235	4148
no. of data/restraints/params	3838/0/272	2530/0/179	4893/0/327
$R1/wR2$ $I > 2\sigma(I)$	0.0348/0.0685	0.0201/0.0456	0.0189/0.0406
$R1/wR2$ (all data)	0.0417/0.0750	0.0247/0.0464	0.0272/0.0418
goodness-of-fit on F^2	1.079	1.051	0.922
largest diff. peak and hole e Å^{-3}	1.95/-1.77	1.43/-1.46	0.87/-0.85

Table 2. Characteristic IR Vibrations of CH_3ReO_3 Fragments (cm^{-1}) in **1**−**7**

MTO	**1**	**2**	**3**	**4**	**5**	**6**	**7**	assignment
1368	1407	1394	1421	1384	1385		1384	CH_3 asym def
1205	1229	1229	1227	1220	1227	1237	1210	CH_3 sym def
998	955	932	958	956	959	955	957	ReO_3 sym str
965	923	925	925	924	918	935	924	ReO_3 asym str
	915	903		905		919	907	
567	548	547	563	541	535	525	542	ReC str
976	931	920	942	928	938	936	929	ReO str averaged

parameters were calculated from the parent carbon/nitrogen atom ($U_{iso(H)} = 1.2/1.5U_{eq(C/N)}$). Full-matrix least-squares refinements were carried out by minimizing $\sum w(F_o^2 - F_c^2)^2$ with the Shelxl-97 weighting scheme. The final residual electron density maps show no remarkable features. *Specials*: **1**: Small extinction effects were corrected with the SHELXL-97 procedure $\varepsilon = 0.0074(2)$. The hydrogen atoms located at the nitrogen atom and the hydroxyl function were found in the final difference Fourier maps and were allowed to refine freely ($d_{N-H} = 0.97(7)$ Å; $d_{O-H} = 0.77(8)$ Å). **6**: Numerical absorption correction was performed after crystal shape optimization with the programs Xshape and Xred (Correction Factors: $T_{min} = 0.1209$, $T_{max} = 0.4016$). Small extinction effects were corrected with the Shelxl-97 procedure $\varepsilon = 0.00055(6)$. The hydrogen atom located at the nitrogen atom was found in the final difference Fourier maps and was allowed to refine freely ($d_{N-H} = 0.81(6)$ Å). **7**: Numerical absorption correction after crystal shape optimization with the programs Xshape and Xred (Correction Factors: $T_{min} = 0.0364$, $T_{max} = 0.5746$). CCDC reference nos. 736275 (**1**), 736274 (**6**), 736276 (**7**).[18a−18h]

Catalytic Reactions. Method A. *cis*-Cyclooctene (343.2 mg, 3.12 mmol), 429 mg of mesitylene (internal standard), H_2O_2 (30% aqueous solution) (0.7 mL, 6.24 mmol), and 1 mol % (31.2 μmol) of compounds **1**−**7** were mixed at 0 °C in 3 mL of CH_2Cl_2.

Method B. *trans*-β-methylstyrene (368.4 mg, 3.12 mmol), 429 mg of mesitylene (internal standard), H_2O_2 (30% aqueous solution) (0.7 mL, 6.24 mmol), and 1 mol % (31.2 μmol) of enantiomerically pure compound **7** were mixed at 0 °C in 3 mL of CH_2Cl_2.

Olefin, mesitylene, and compounds **1**−**7** as catalysts were added to the reaction vessel under standard conditions. The reaction began with the addition of H_2O_2. The course of the reaction was monitored by quantitative GC analysis. Samples were taken at regular time intervals, diluted with CH_2Cl_2, and treated with a catalytic amount of $MgSO_4$ and MnO_2 to remove water and to destroy the excess of peroxide. The resulting slurry was filtered, and the filtrate injected into a (or chiral) GC column. The conversion of cyclooctene and the formation of cyclooctene oxide were calculated from calibration curves ($r^2 = 0.999$) recorded prior to the reaction course.

Computational Details. All calculations were performed with GAUSSIAN-03[19] using the density functional/Hartree−Fock hybrid model Becke3LYP[20] and the split valence double-ζ

(18) (a) *CrysAlis, Data Collection Software and Data Processing Software for Oxford Xcalibur diffractometer*, Version 1.171; Oxford Diffraction Ltd.: Oxfordshire, U.K., 2005. (b) *Xarea, Data Collection Software and Data Processing Software for Stoe IPDS 2T diffractometer*, Version 1.26; Stoe & Cie: Darmstadt, Germany, 2004. (c) *Xshape, Xred, Data Processing Software for Stoe IPDS 2T diffractometer*, Version 1.26; Stoe & Cie: Darmstadt, Germany, 2004. (d) *Sir92* Altomare, A.; Cascarano, G.; Giacovazzo, C.; Guagliardi, A.; Burla, M. C.; Polidori, G.; Camalli, M. *J. Appl. Crystallogr.* **1994**, *27*, 435–436. (e) *International Tables for Crystallography*; Wilson, A. J. C., Ed.; Kluwer Academic Publishers: Dordrecht, The Netherlands, 1992; Vol. C, Tables 6.1.1.4, 4.2.6.8, and 4.2.4.2. (f) Sheldrick, G. M. *Shelxl-97*; Universität Göttingen: Göttingen, Germany, 1998. (g) Spek, A. L. *Platon: A Multipurpose Crystallographic Tool*; Utrecht University: Utrecht, The Netherlands, 2007. (h) Farrugia, L. J. *WinGX*, Version 1.70.01, January 2005; *J. Appl. Crystallogr.* **1999**, *32*, 837−838.

(19) Frisch, M. J.; Trucks, G. W.; Schlegel, H. B.; Scuseria, G. E.; Robb, M. A.; Cheeseman, J. R.; Montgomery, J.; Vreven, J. A. T.; Kudin, K. N.; Burant, J. C.; Millam, J. M.; Iyengar, S. S.; Tomasi, J.; Barone, V.; Mennucci, B.; Cossi, M.; Scalmani, G.; Rega, N.; Petersson, G. A.; Nakatsuji, H.; Hada, M.; Ehara, M.; Toyota, K.; Fukuda, R.; Hasegawa, J.; Ishida, M.; Nakajima, T.; Honda, Y.; Kitao, O.; Nakai, H.; Klene, M.; Li, X.; Knox, J. E.; Hratchian, H. P.; Cross, J. B.; Bakken, V.; Adamo, C.; Jaramillo, J.; Gomperts, R.; Stratmann, R. E.; Yazyev, O.; Austin, A. J.; Cammi, R.; Pomelli, C.; Ochterski, J. W.; Ayala, P. Y.; Morokuma, K.; Voth, G. A.; Salvador, P.; Dannenberg, J. J.; Zakrzewski, V. G.; Dapprich, S.; Daniels, A. D.; Strain, M. C.; Farkas, O.; Malick, D. K.; Rabuck, A. D.; Raghavachari, K.; Foresman, J. B.; Ortiz, J. V.; Cui, Q.; Baboul, A. G.; Clifford, S.; Cioslowski, J.; Stefanov, B. B.; Liu, G.; Liashenko, A.; Piskorz, P.; Komaromi, I.; Martin, R. L.; Fox, D. J.; Keith, T.; Al-Laham, M. A.; Peng, C. Y.; Nanayakkara, A.; Challacombe, M.; Gill, P. M. W.; Johnson, B.; Chen, W.; Wong, M. W.; Gonzalez, C.; Pople, J. A. *Gaussian03*, Rev. C.02; Gaussian Inc.: Wallingford, CT, 2004.

(20) (a) Vosko, S. H.; Wilk, L.; Nusair, M. *Can. J. Phys.* **1980**, *58*, 1200–1211. (b) Lee, C.; Yang, W.; Parr, R. G. *Phys. Rev. B.* **1988**, *37*, 785–789. (c) Becke, A. D. *J. Chem. Phys.* **1993**, *98*, 5648–5652.

Chart 1. MTO Salen Complexes **1**−**7**

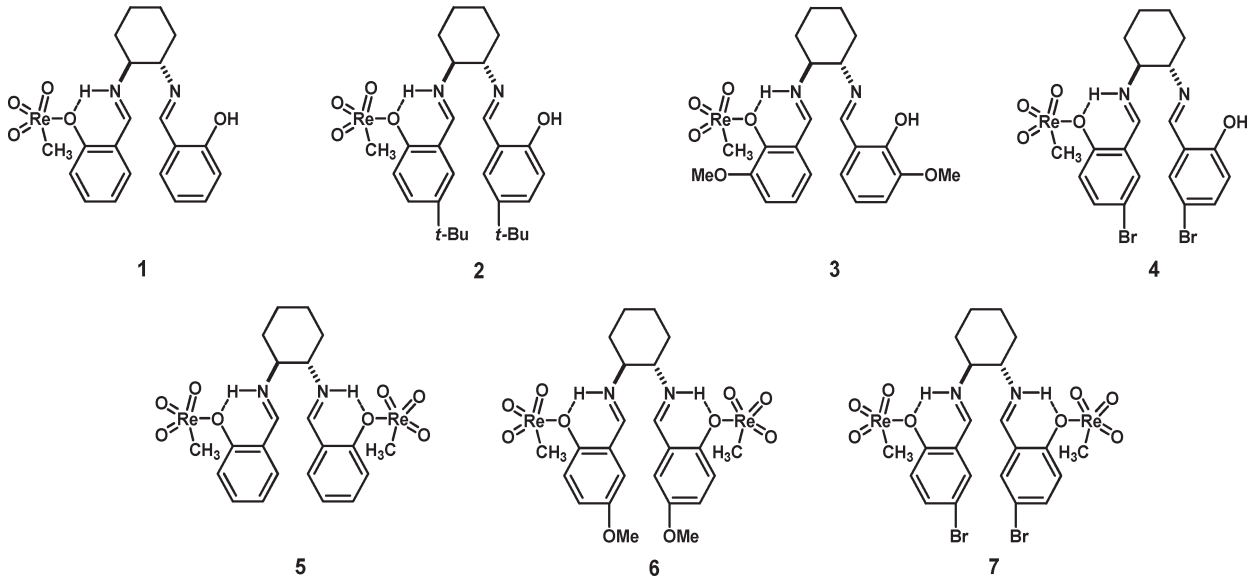

(DZ) basis set 6-31G*.[21] The Re atoms were described with a Hay−Wadt ECP[22] with a DZ description of the valence electrons. No symmetry or internal coordinate constraints were applied during optimizations. All reported intermediates were verified as being true minima by the absence of negative eigenvalues in the vibrational frequency analysis. Structural depictions were obtained with the program GaussView.[23]

Results and Discussion

Synthesis and Spectroscopic Characterization. A series of salen compounds was synthesized using methods described in the literature,[16] and their role as ligands examined. Complexes **1**−**4** were formed by mixing the corresponding salen ligands and MTO in a 1:1 ratio in Schlenk tubes at 23 °C in diethyl ether. Complexes **5**−**7** were prepared by treating 2 equiv of MTO with the ligand in the same solvent at −30 °C (**5** and **6**) and 23 °C (**7**) (see Scheme 1). The yellow (**1**−**4**, **7**), yellow-green (**5**), or red (**6**) complexes can be easily isolated by crystallization from Et_2O and purified by washing with *n*-hexane (Chart 1). In air at room temperature, complexes **1**−**4** and **7** show good stability both in the solid state and in solution. However, they are somewhat sensitive to moisture and elevated temperatures. Complexes **5** and **6** are thermally unstable and decompose to brownish residues at room temperature within a few hours. They must be kept at −30 °C under an argon atmosphere to achieve a longer storage time and to avoid decomposition. Complexes **1**−**7** display similar solubilities. They are all soluble in most polar organic solvents such as CH_2Cl_2, EtOH, acetone, CH_3CN, and tetrahydrofuran (THF).

An attempt to synthesize a MTO complex using L**6** as the ligand failed. Only free MTO and free ligand could be isolated from the reaction mixture. This might, at least in part, be due to the comparatively strong electron-withdrawing capability of the two bromine substituents, rendering the ligand a poor electron donor. Even more importantly, Br subsitutents are *ortho* to the potentially co-ordinating hydroxy groups making the environment of the coordination site of the Schiff base ligand more hindered and reducing the ability of MTO to coordinate with the oxygen atom of the −OH group. When L**2** and L**3** were treated with two (or more) equiv MTO, compounds **2** and **3** were obtained with only one MTO molecule in the complexes (see Chart 1). Nevertheless, L**4** only forms the 2:1-ratio complex **6** with MTO and L**1** and L**5** form both mono- and bis- coordination modes resulting in the corresponding complexes **1**, **4**, **5**, and **7**.

In the IR spectra, the Re=O bands of compounds **1**−**7** are found in the region 903−959 cm^{-1}. These bands are red-shifted in comparison to free MTO (see Table 2) because of the additional electron density donated by the ligand to the rhenium center. Accordingly, the Re=O bonds are considerably weakened. A small splitting of the asymmetric ReO_3 stretching band can be seen for most compounds because of the complex symmetry. However, such a splitting is not observed in compounds **3** and **5**, most likely because the difference is too small to be clearly visible in the IR spectra. The average Re=O stretching bands vary from 920 to 942 cm^{-1}. In comparison to the values of many other MTO Schiff base complexes (950−960 cm^{-1}), the red-shifts observed here are comparatively large, revealing a stronger coordination between MTO and the salen ligands in the solid state.[9] The L**2** derived compound **2** displays the biggest red-shift of Re=O bands (56 cm^{-1}) owing to the strong donor *t*-butyl group on the ligand.

The proton of one phenol group of the free salen ligands moves to the nitrogen atom of the imine group after complexation. The −CH=N group frequencies, usually in the range of 1626−1632 cm^{-1} for free ligands, are observed at higher wave numbers (ca. 1635−1651 cm^{-1}) after complexation in the case of compounds **1**−**7** because

(21) (a) Hehre, W. J.; Ditchfield, R.; Pople, J. A. *J. Chem. Phys.* **1972**, *56*, 2257–2261. (b) Francl, M. M.; Petro, W. J.; Hehre, W. J.; Binkley, J. S.; Gordon, M. S.; DeFrees, D. J.; Pople, J. A. *J. Chem. Phys.* **1982**, *77*, 3654–3665.

(22) (a) Hay, P. J.; Wadt, W. R. *J. Chem. Phys.* **1985**, *82*, 270–283. (b) Hay, P. J.; Wadt, W. R. *J. Chem. Phys.* **1985**, *82*, 299–310.

(23) Dennington, R., II; Keith, T.; Millam, J. *GaussView*, Version 4.1; Semichem Inc.: Shawnee Mission, KS, 2007.

Table 3. Selected IR (KBr) Data (cm^{-1}) for Compounds **1**−**7**[a]

	imine group[b]	phenolic OH group and coupled ring vibrations[b]				
compound	$\nu_{(C=N)}$	β(OH)	$\nu_{(CX)}$	$\nu_{(CX)}$	$\nu_{(CX)}$	γ(OH)
$C_{20}H_{22}N_2O_2$	1630 vs	1341 m, sh	1280 s	1147 m, sh	846 s	768 s
$C_{20}H_{22}N_2O_2 \cdot CH_3ReO_3$ (**1**)	1646 s, br	1348 m, br	1267 m	1148 m, sh	848 w	
$C_{20}H_{22}N_2O_2 \cdot 2CH_3ReO_3$ (**5**)	1651vs					
$C_{28}H_{38}N_2O_4$	1631 vs	1361 m, sh	1267 s	1092 m	825 s	786 m
$C_{28}H_{38}N_2O_4 \cdot CH_3ReO_3$ (**2**)	1636 vs	1363 m	1269 s	1092 m	825 s	791 m
$C_{20}H_{26}N_2O_4$	1626 s		1254 s	1091 s	859 w	729 s
$C_{20}H_{26}N_2O_4 \cdot CH_3ReO_3$ (**3**)	1645 s		1254 vs	1096 m	853 m	
$C_{20}H_{26}N_2O_4$	1628 vs	1329 m, sh	1270 vs	1098 m	821 s	760 m, sh
$C_{20}H_{26}N_2O_4 \cdot 2CH_3ReO_3$ (**6**)	1635 s					
$C_{20}H_{20}Br_2N_2O_2$	1632 vs	1368 s	1281 s	1093 m, sh	862m, sh	698 m, sh
$C_{20}H_{20}Br_2N_2O_2 \cdot CH_3ReO_3$ (**4**)	1649 vs	1368 m	1280 s	1093 m	863 m	698 m, br
$C_{20}H_{20}Br_2N_2O_2 \cdot 2CH_3ReO_3$ (**7**)	1650 vs					

[a] The respective pure ligand vibrations are given for the sake of comparison. [b] Notation of vibrational modes: υ(C=N), C=N stretching; β(OH), hydrogen bonded OH in-plane deformation; $\upsilon_{(CX)}$, substituent sensitive aromatic ring stretchings; γ(OH) phenolic out-of-plane vibrations. Notation of peak intensity: vs (very strong); s (strong); m (medium); w (weak), br (broad), sh (sharp).

Table 4. Selected ^{1}H and ^{13}C NMR Spectroscopic Data for Compounds **1**−**7** in $CDCl_3$

	MTO−CH_3	
compound	δ (^{1}H)	δ (^{13}C)
MTO	2.67	19.0
1	2.58	19.7
2	2.54	20.2
3	2.59	19.5
4	2.60	19.5
5	2.61	19.4
6	2.59	19.6
7	2.60	19.4

Table 5. Temperature-Dependent ^{1}H-NMR Determination of Compounds **4** and **7**

	δ_{ReCH3}/(ppm)			δ_{X-H}/(ppm)		
temperature (°C)	MTO	**4**	**7**	**L5**$_{(X = O)}$	**4**$_{(X = O, N)}$	**7**$_{(X = N)}$
−60	2.74	2.35	2.37	13.52	13.49	13.49
−40	2.70	2.51	2.52	13.44	13.43	13.42
−20	2.67	2.58	2.58	13.35	13.35	13.35
0	2.66	2.59	2.59	13.27	13.27	13.27
20	2.65	2.60	2.60	13.19	13.18	13.19
40	2.62	2.60	2.60	13.11	13.16	13.17
60	2.60	2.61	2.61	13.04	13.12	13.14

of the proton transfer from the OH group to the imine group (see Table 3). As further evidence of the existence of the proton transfer after complexation, the distances of O−H and N−H bonds for both the coordinated and uncoordinated moieties of complex **1** are clearly different according to X-ray analysis (see below for more details).

In the case of complexes **1**−**4** with one MTO molecule coordinated, the differences between the functional group vibrations of coordinated and non-coordinated parts of the ligands are visible. The coupled ring frequencies in the range of 1091 to 1148 cm^{-1} show the influence of the (remaining) uncoordinated −OH moiety still (see Table 3). In the case of the 2:1 adducts, the original ligand vibrations of the hydroxyl moiety disappear.

The ^{1}H and ^{13}C NMR data of the $ReCH_3$ groups of compounds **1**−**7** are shown in Table 4. The proton signals of the Re-CH_3 moiety of compounds **1**−**7** are slightly shifted (0.06−0.13 ppm) to high field compared to non-coordinated MTO, indicating a weak MTO−salen interaction in solution at room temperature. Similarly, a small change in chemical shift (0.4−1.2 ppm) for the Re−C bond (carbon atom of the methyl group) in compounds **1**−**7** can be observed in the ^{13}C NMR-spectra. In the case of compound **2**, possibly owing to the *tert*-butyl groups on the salen compound acting as electron donors, the shift changes observed for the Re-CH_3 moiety, both in the ^{1}H and ^{13}C NMR spectra are larger than those observed for the other compounds.

The temperature-dependent proton NMR studies of compounds **4** and **7** reflect the fact that the coordination between ligand and MTO becomes stronger at lower temperatures (see Table 5). In the experiments, free MTO, salen ligand, and the mixture of MTO and ligand for compounds **4** and **7** in 1:1 or 2:1 ratio were measured initially at −60 °C in $CDCl_3$, with a subsequent, stepwise increase in the temperature to 60 °C. For the 1:1 and 2:1 mixtures, no significant differences of the chemical shifts with respect to the functional groups of the complexes are observed in the spectra. It is seen that the $ReCH_3$ chemical shift of free MTO is located at 2.74 ppm at −60 °C. After adding 1 or 1/2 equivalents of ligand, however, the proton signals of $ReCH_3$ are shifted to 2.35 and 2.37 ppm, proving a coordination of the ligand to MTO under formation of the complexes **4** and **7**. The chemical shift changes (ca. 0.4 ppm) of $ReCH_3$ are much larger than those at room temperature (0.07 ppm), indicating a stronger coordination at −60 °C between the ligand and MTO. While increasing the temperature, the Re-CH_3 signal shifts to high field both in the case of compounds **4** and **7** and finally appears at 2.61 ppm at 60 °C. A significant change is observed from −60 °C to −40 °C where the signal shifts from 2.35 (2.37) to 2.51 (2.52) ppm. The proton signals of OH (or NH) group have a similar chemical shift behavior with respect to a comparison between the free ligand and the ligated complexes **4** and **7** at room and low temperatures. While raising the temperature, the proton signals shift to high field. The proton peaks appear at 13.52 ppm (**L5**) and 13.49 ppm (**4**, **7**) at −60 °C. They shift to 13.04 (**L5**), 13.12 (**4**), and 13.14 (**7**) ppm at 60 °C. A chemical shift difference (ca. 0.08−0.1 ppm) between **L5** and **4**, **7** at 60 °C is observed. However, in the case of the 1:1 adducts, two independent

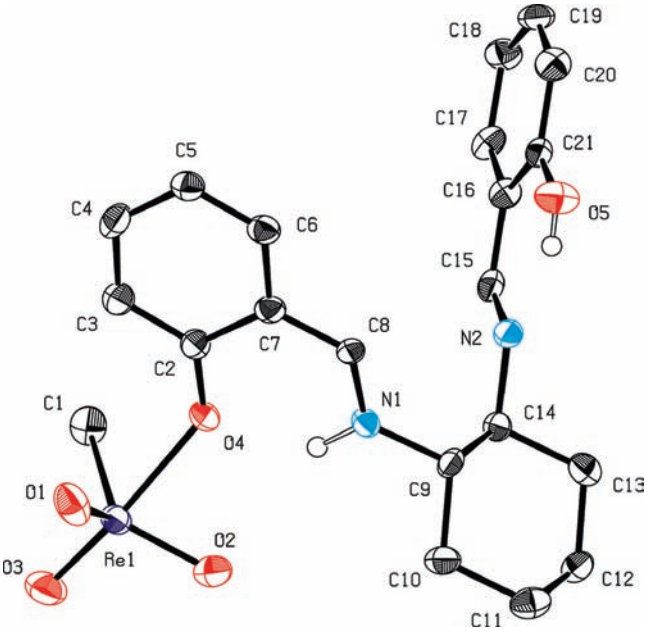

Figure 1. PLATON view of the solid-state structure of complex **1**. The thermal ellipsoids are shown at the 50% probability level. Hydrogen atoms are omitted for clarity.

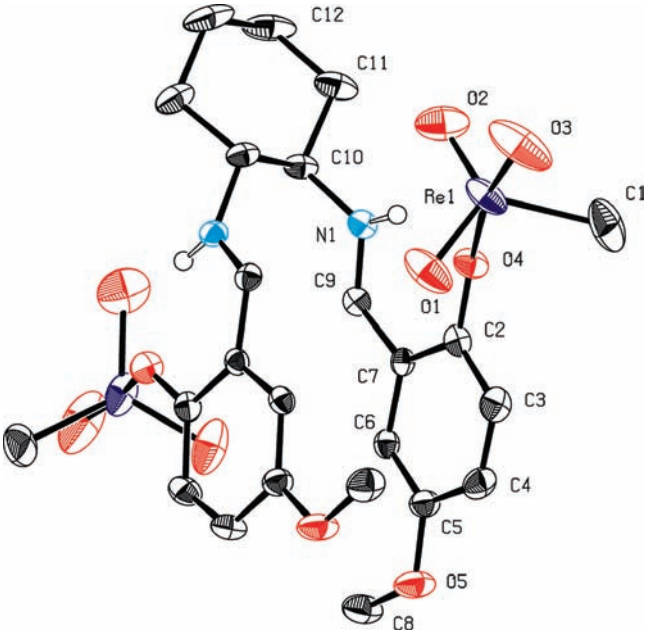

Figure 2. PLATON view of the solid-state structure of complex **6**. The thermal ellipsoids are shown at the 50% probability level. Hydrogen atoms are omitted for clarity. The molecule is located on a 2-fold axis. Symmetry operation for equivalent atoms: (2.555) $-x, y, 1/2-z$.

peaks representing the coordinated NH and the uncoordinated OH proton cannot be observed even at − 60 °C. The temperature changes only influence the line width of the signals, but do not lead to two separate signals for the 1:1 adducts at low temperature. This observation might indicate a rapid position change of the MTO molecule between the two sites of the ligand in the 1:1 adducts even at low temperatures in solution. This is also supported by the fact that the 2:1 adducts exhibit sharp peaks in the OH region at temperatures between −60 and 60 °C, which

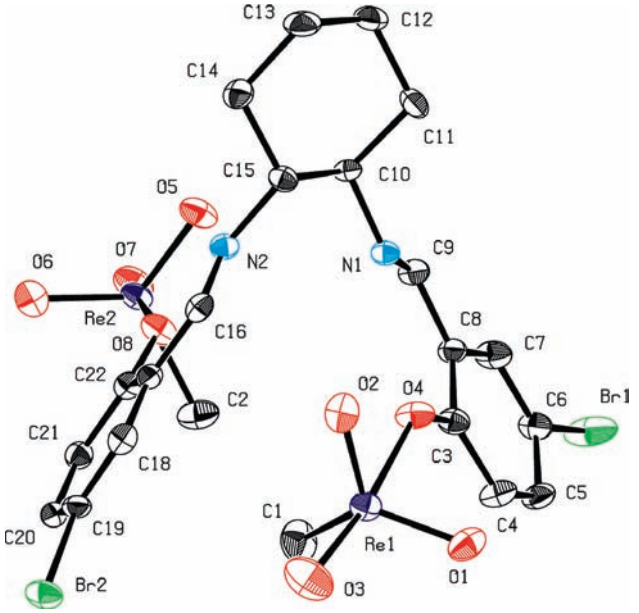

Figure 3. PLATON view of the solid-state structure of complex **7**. The thermal ellipsoids are shown at the 50% probability level. Hydrogen atoms are omitted for clarity.

Table 6. Selected X-ray and DFT Calculated Bond Lengths (Å) of Compounds **1**, **6**, and **7**

	1		**6**		**7**	
	X-ray	DFT	X-ray	DFT	X-ray	DFT
Re1−O1	1.710(5)	1.7161	1.709(3)	1.7139	1.711(4)	1.732
Re1−O2	1.706(4)	1.7294	1.709(4)	1.7334	1.724(4)	1.712
Re1−O3	1.701(5)	1.7079	1.698(4)	1.7068	1.699(4)	1.704
Re1−O4	2.201(4)	2.3905	2.181(3)	2.4043	2.184(3)	2.491
Re1−C1	2.111(7)	2.1190	2.114(6)	2.1158	2.122(5)	2.106
Re2−O5					1.715(3)	1.729
Re2−O6					1.721(3)	1.714
Re2−O7					1.712(4)	1.706
Re2−O8					2.169(3)	2.450
Re2−C2					2.126(5)	2.113

nicely shows that here, the MTO complexes do not exchange at the NMR time scale.

The elemental analysis results clearly show a 1:1 coordination between the ligands and MTO for compounds **1**−**4** but a 1:2 coordination for compounds **5**−**7**.

The CI mass spectra show the peaks of the Schiff base ligands and MTO separately for compounds **1**−**3**, **6**. The molecular peak (M+2) can be only observed for compound **4**. In the case of compounds **5** and **7**, a peak indicating the loss of one MTO molecule from the complete molecule, as well as a peak for the free ligand (after having lost both MTO moieties), can be observed.

X-ray Crystal Structures of Compounds 1, 6, 7. The molecular structures of the examined compounds are shown in Figures 1−3, and the selected bond lengths and angles are summarized in Tables 6 and 7. The rhenium center(s) in each compound displays a distorted trigonal-bipyramidal geometry. Notably, all three structures show a *cis* arrangement with respect to the methyl group of MTO to the salen ligand. In the structures, the methyl group and two oxygen atoms occupy the equatorial positions while the donating phenolic group and the

Table 7. Selected X-ray and DFT Calculated Bond Angles (deg) of Compounds **1**, **6**, and **7**

	1		**6**		**7**	
	X-ray	DFT	X-ray	DFT	X-ray	DFT
O1−Re1−O2	119.2(2)	118.6	119.3(2)	118.7	119.0(2)	118.7
O1−Re1−O3	103.4(3)	105.4	103.6(2)	105.6	103.7(2)	106.4
O1−Re1−O4	84.0(2)	80.3	83.8(1)	80.4	85.7(2)	75.5
O1−Re1−C1	116.8(3)	115.3	117.3(2)	114.8	114.3(2)	113.3
O2−Re1−O3	103.6(2)	106.8	104.1(2)	105.7	103.0(2)	106.4
O2−Re1−O4	79.4(2)	77.7	80.4(1)	77.9	79.4(1)	78.5
O2−Re1−C1	116.8(2)	114.1	115.7(2)	114.6	119.9(2)	113.6
O3−Re1−O4	168.9(2)	170.0	167.5(2)	169.7	167.1(2)	172.3
O3−Re1−C1	89.7(2)	93.3	89.6(2)	92.9	89.2(2)	94.9
O4−Re1−C1	79.5(2)	76.8	78.0(2)	76.9	78.8(2)	77.6
Re1−O4−C2	134.2(4)	134.9	132.3(2)	132.2		
Re1−O4−C3					134.2(3)	133.6
O5−Re2−O6					119.1(2)	118.3
O5−Re2−O7					102.6(2)	106.2
O5−Re2−O8					79.3(1)	76.5
O5−Re2−C2					117.2(2)	113.7
O6−Re2−O7					103.6(2)	106.1
O6−Re2−O8					84.2(1)	79.2
O6−Re2−C2					117.0(2)	114.4
O7−Re2−O8					169.4(2)	171.2
O7−Re2−C2					89.4(2)	94.4
O8−Re2−C2					80.5(2)	76.9
Re2−O8−C22					135.9(3)	134.3

remaining oxygen reside in the apical sites. Packing effects might be responsible for the *cis* arrangement.

Compound **6** displays a symmetrical structure. The symmetry operation for equivalent atoms is (2.555) − *x*, *y*, 1/2 − *z*. The Re−C distance for compounds **1**, **6**, and **7** are 2.111(7) Å, 2.114(6) Å, and 2.122 (5)Å (*2.126(5)*) *Å*, respectively. The values are slightly longer than that in free MTO (2.060(9) Å).[3h] The Re═O bond lengths in complexes **1**, **6** and **7** are around 1.7 Å as observed in all published MTO and MTO *N*- or *O*- donor adduct.[3h,7−9] The respective Re−O bond distances are 2.201(4) (1), 2.181(3)(6), and 2.184(3) (*2.169(3)*) Å (7). The Re−O bonds are similar to those in all MTO Schiff base complexes that have previously measured (2.17−2.30 Å).[9] In the crystal structure of complex **1**, the bond distances of N2−H5 (lying in the uncoordinated moiety of the compound) is 1.91(8) Å whereas O4−H1 (lying in the coordinated moiety) is 1.82(6) Å (see Supporting Information). The bond distances of O5−H5 and N1−H1 are 0.77(8) and 0.97(7) Å, respectively. Obviously, the O−H bond becomes longer while the N−H bond becomes shorter after MTO coordination, indicating a proton transfer from the OH group to the imine group of the ligand. The distortion of the trigonal-bipyramidal structure can be observed through the value of the O═Re═O angles of the complexes. If no distortion occurred, the value should be 180° (the three atoms should reside in one line on the apical axis of the trigonal-bipyramidal), but in the case of compounds **1**, **6**, and **7** the values are 168.9(2)°, 167.5(2)°, and 167.1 (2)° (*169.4 (2)*°), respectively.

DFT-Computed Geometries for Compounds 1−7 and Computational Considerations on the Adduct Formation. Because of the difficulties in crystallizing complexes **2**−**5**, the possible geometries for these complexes (as well as **1**, **6**, and **7**) were calculated to get an insight of a probable structure. The calculated bond distances and bond angles

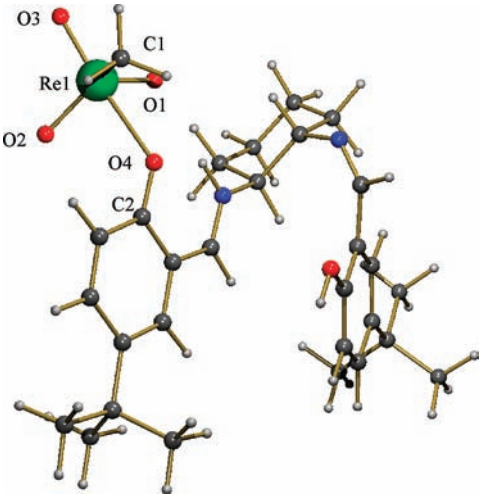

Figure 4. Optimized structure of complex **2**.

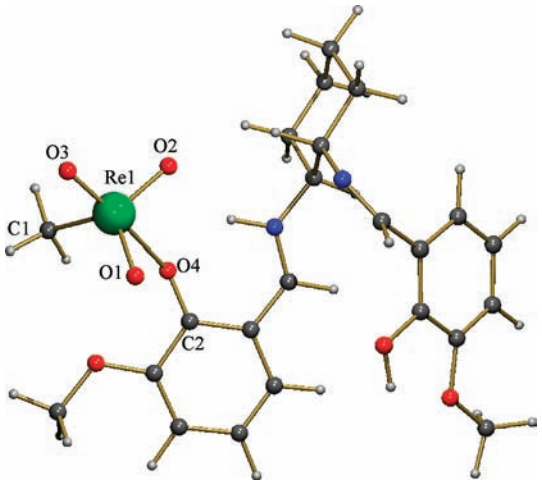

Figure 5. Optimized structure of complex **3**.

from DFT-optimized structures (B3LYP/6-31G* with Re-ECP) for compounds **1**, **6**, and **7** are included in the Tables 6 and 7 to enable comparison with those obtained from X-ray crystallography. It can be observed that, with exception of the Re1−O4 distance between Re and the Schiff base, all calculated and measured bond distances are equal within an error range of 0.03 Å, and the bond angles shown in Table 6 are accurate to within 5 degrees. The reason for the greater discrepancy for Re1−O4 originates, on the one hand, from the difference between a solid state structure and a gas-phase structure as calculated by DFT, and on the other hand, from the B3LYP methodology, which describes well covalent bonds but less-well coordinative interactions such as the Re1−O4 interaction. In such a case, it tends to overestimate the distance between the atoms.

The DFT-optimized structures for complexes **2**−**5** and the assumed 1:1 MTO complex of L**4** are shown in Figures 4−8. Relevant bond-lengths and angles for **2**−**5** are listed in Tables 8 and 9, respectively. Compounds **2**−**4** have been identified as 1:1 complexes of MTO and the corresponding salen ligands (according to elemental analysis and mass spectrometry), while complex **5** is an adduct of two molecules MTO and the salen moiety.

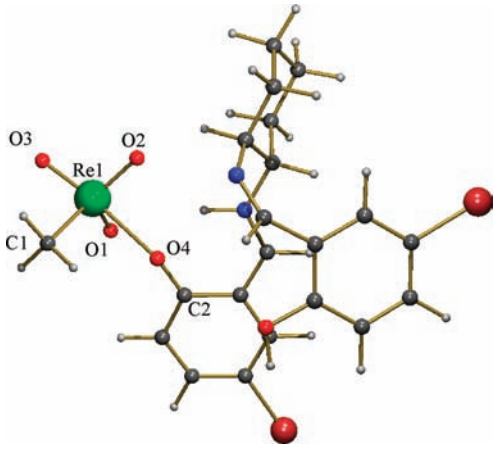

Figure 6. Optimized structure of complex **4**.

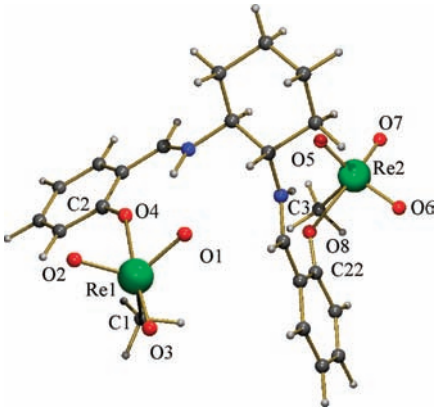

Figure 7. Optimized structure of complex **5**.

To find a reason for the different complex formation behavior of the various salen ligands, geometries of the free salen ligands were also optimized (see Supporting Information), and all possible mono- and bis-MTO complex formation energies for the different complexes were computed using DFT and compared.

As can be seen from Table 10, the addition of the first molecule of MTO is endergonic in all cases. The addition of ligand **L6** to MTO bearing two bromide atoms on each ring is the most endergonic reaction (and is not observed experimentally). This result supports the above-mentioned deactivation caused by the electronic effect of the Br moieties. The second step, namely, the formation of a bis-adduct, is exergonic, leading to, for all systems, a negative overall free energy change for both steps together. In light of this information, all the bis-complexes might be synthetically feasible. Therefore, the thermodynamics, in this case the free energies of the complexation reactions, do not provide an explanation as to why the addition of MTO leads to a mono- rather than to a bis-product.

Steric hindrance from the functional groups at the aromatic rings of the salen ligands may play a role in preventing or allowing the addition of a second MTO moiety. To give an example we compared the mono-MTO complexes of the two isomers **L3** (R = OMe, R′ = H) and **L4** (R = H, R′ = OMe). In the case of **L4**, the mono-complex cannot be observed because of the immediate formation of a bis-complex, even in the absence of excess

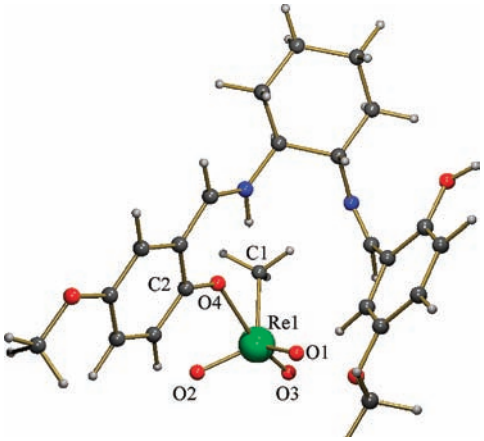

Figure 8. Optimized structure of the 1:1 MTO complex of ligand **L4**.

Table 8. DFT Calculated Bond Lengths (Å) of Compounds **2**–**5** Based on the Optimized Structures

	2	**3**	**4**	**5**
Re1–O1	1.717	1.713	1.715	1.714
Re1–O2	1.729	1.728	1.727	1.734
Re1–O3	1.706	1.707	1.706	1.708
Re1–O4	2.376	2.474	2.457	2.357
Re1–C1	2.121	2.107	2.111	2.122
Re2–O5				1.715
Re2–O6				1.734
Re2–O7				1.707
Re2–O8				2.364
Re2–C2				2.120

Table 9. DFT Calculated Bond Angles (deg) of Compounds **2**–**5** Based on the Optimized Structures

	2	**3**	**4**	**5**
O1–Re1–O2	118.4	118.6	118.6	119.8
O1–Re1–O3	105.3	106.3	106.1	105.7
O1–Re1–O4	80.7	79.5	79.1	82.7
O1–Re1–C1	115.2	114.4	114.3	114.1
O2–Re1–O3	105.7	106.1	106.3	104.5
O2–Re1–O4	78.1	75.2	76.2	75.8
O2–Re1–C1	114.1	113.4	113.4	115.5
O3–Re1–O4	169.4	171.9	171.5	169.6
O3–Re1–C1	93.9	94.3	94.5	92.0
O4–Re1–C1	75.5	78.0	77.1	78.8
Re1–O4–C2	134.2	135.2	135.0	
Re1–O4–C3				142.8
O5–Re2–O6				118.8
O5–Re2–O7				105.4
O5–Re2–O8				80.9
O5–Re2–C2				114.9
O6–Re2–O7				105.4
O6–Re2–O8				77.3
O6–Re2–C2				115.1
O7–Re2–O8				170.2
O7–Re2–C2				92.6
O8–Re2–C2				77.7
Re2–O8–C22				137.9

MTO. However, in the case of **L3**, the reaction stops after formation of a 1:1 adduct. The 1:1 complex (Figure 5) shows that in the optimized geometry the OH-group which should be attacked by the second MTO, is blocked by the neighboring –OMe group and additionally covered from below by the other side of the salen ligand. The 1:1 complex of ligand **L4** (Figure 8) reveals that the –OH group of the free site is differently oriented. The –OH group points away from the complex and has no steric

Table 10. Free Energies (kcal/mol) of Formation of the Two Steps of Complexation

Ligand (R,R′)	ΔG (1st step)	ΔG (2nd step)	ΔG (both steps)	obtained complex (Ligand:MTO)
L1 (H,H)	+3.0	−19.2	−16.2	1:1, 1:2
L2 (H,*t*-Bu)	+1.7	−19.8	−18.1	1:1
L3 (OMe,H)	+6.4	−14.4	−8.0	1:1
L4 (H,OMe)	+0.6	−8.1	−7.4	1:2
L5 (H,Br)	+2.6	−19.5	−16.9	1:1, 1:2
L6 (Br,Br)	+7.4	−17.7	−10.4	no reaction

interference with neighboring groups or the other side chain of the ligand. Therefore, the −OH moiety can easily react with a second MTO to form a bis-MTO complex, as it was observed experimentally.

Applications as Epoxidation Catalysts. Compounds **1**−**7** were examined as catalysts for the epoxidation of cyclooctene with hydrogen peroxide (see Figure 9) using CH_2Cl_2 as solvent. Further details of the catalytic reaction are given in the experimental section. Blank reactions showed that no significant amounts of epoxide are formed in the absence of catalysts. A catalyst/oxidant/substrate ratio of 1:200:100 was used in all experiments. No significant formation of byproduct (e.g., diol) was observed. All catalytic reactions follow first order kinetics in which the reaction conversion increases steadily for the first 2 h and then slows down.

After adding the oxidant H_2O_2, the yellow solution became darker, indicating a formation of the active species of the catalysts. In general, however, most of the compounds, with the exception of complex **7**, show only moderate or low catalytic activity during the first 4 h (with epoxide yields lower than 60%) for cyclooctene epoxidation. The catalytic activity, in most cases, is generally lower than that of free MTO (Figure 9) in contrast, for example, to the highly active Schiff base adducts of MTO published before.[9a] There were no further (obvious) changes of the epoxide yield even after 24 h. This might be due to the cyclohexane ring originating from the Schiff base ligands increasing the basicity of the Schiff base ligands, thus decreasing the acidity of the MTO Re atom; accordingly, the catalytic activity of the complexes is reduced. In addition, the basic salen ligand might accelerate catalyst decomposition during the reactions.[9a] In the case of complexes **1**−**3**, **5**, and **6**, the yellow catalytic solution containing the active species of monoperoxo and bis-peroxo complexes becomes white after 4 h, and the color does not change even upon addition of more H_2O_2 to the solution, reflecting decomposition of the active species. To slow down the decomposition of active species, all the catalytic reactions were followed at 0 °C in the experiments. Not unexpectedly, it is observed that the compounds bearing electron-withdrawing groups display higher catalytic activity than the ones with electron-donating substituents. Conversely, the higher the electron-donating ability, the lower the activities of the catalysts. For the 1:1 ratio complexes, the epoxide yields are **2** < **3** < **1** < **4**, whereas **6** < **5** < **7** for the 2:1 ratio complexes. L**5** (Br substitution) derived compound **7** show highest activity, with 88% epoxide yield after 24 h. However, L**2** (*t*-butyl substituted) derived compound **2** shows the lowest catalytic activity (9.8%) among the examined mono- complexes. Despite most of complexes exhibiting only moderate catalytic activity, all of them show high epoxidation selectivity (>99%) and the

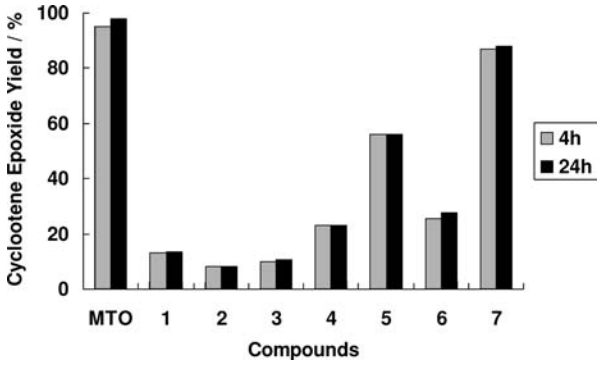

Figure 9. Yield of the cyclooctene epoxidation after 4 h (gray bars) and after 24 h (black bars) in the presence of MTO and the complexes **1**−**7** as catalysts at 0 °C with 1 mol % catalyst.

diol side product was not observed in the GC during any of the reactions.

It has to be noted that the epoxide yield of compounds **5** and **7** are more than double those of the respective yields of compounds **1** and **4** at any given time. Accordingly, the activity difference cannot solely be ascribed to there being double the number of active centers in the case of compounds **5** and **7**. The second MTO moiety acts (besides its catalytic activity) as an electron-withdrawing group, thus enhancing the catalytic activity of the 2:1 compounds (**5**, **7**) in comparison to the 1:1 compounds (**1**, **4**). A coordination of one salen ligand with two MTO molecules therefore leads to an additional "ligand enhanced" catalytic activity of the system (ligand acceleration).

A further catalytic experiment using the prochiral olefin "*trans*-β-methylstyrene" as substrate was also carried out to investigate the potential for asymmetric catalytic ability of the complexes. Therefore, the most active complex **7** was chosen in this case, and the enantiomerically pure compound was used as catalyst. A catalyst/oxidant/substrate ratio of 1:200:100 was applied at 0 °C in CH_2Cl_2 solution. The epoxide yield reaches 92% after 24 h; however, the obtained enantiomeric excess value (ee) is only 10%. The low ee obtained may be due to the fluxionality of the Re-ligand bond or to the distant location of the chiral centers to the peroxo ligands of the active species. More work will be necessary to establish the mechanism of the catalytic reaction and the exact location where the oxygen transfer takes place.

Conclusions

A new class of MTO adducts has been synthesized, consisting of MTO and a salen based ligand. The MTO salen complexes with one or two MTO molecules coordinated can be easily prepared, in several cases by varying

the ratio of metal to ligand in the reaction. DFT optimized molecular structures of the mono- MTO complexes suggested that steric hindrances may be preventing the addition of a second MTO moiety to form bis- MTO complexes for some ligands. Compounds **1**−**5** and **7** show good stability both in the solid state and in solution, while compound **6** needs to be kept at −30 °C under an argon atmosphere. The solid-state structures of the complexes show distorted trigonal-bipyramidal structures with the methyl group of MTO residing in the apical sites in the *cis* position because of the packing effect of the molecules. In the reaction of the salen compounds and MTO, the Lewis acidic rhenium(VII) is coordinated to O^-, while the phenolic proton of the ligand is transferred to a ligand imine group. In solution, the complexes undergo a fast metal−ligand exchange, this being responsible for low ee's when using a chiral Re complex as epoxidation catalyst with prochiral olefins. The catalytic performance of MTO salen complexes is, as usual, largely affected by the ring substituents. However, bis-MTO complexes show an disproportionately high catalytic activity, most likely because of the presence of a second MTO molecule, reacting not only as a second catalytic center but also as a strongly electron withdrawing moiety on the ligand.

Acknowledgment. Z.X. and H.C.-M. thank the Alexander von Humboldt foundation for postdoctoral fellowships; M.-D.Z. acknowledges the International Graduate School of Science and Engineering for a Ph.D. Grant.

Supporting Information Available: The combined CIF files for crystallographic data, *XYZ* coordinates of the optimized ligand molecules and complexes together with absolute energies. This material is available free of charge via the Internet at http://pubs.acs.org.